

Curvature in conformal mappings of 2D lattices and foam structure

BY ADIL MUGHAL (1,2) AND DENIS WEAIRE (3,4)

(1) *ISI Foundation, Viale S. Severo 65, 10133 Torino, Italy* (2) *Institute of Mathematics and Physics, Aberystwyth University, SY23 3BZ, UK.* (3) *Université Paris-Est, Laboratoire de Physique des Matériaux Divisés et des Interface, UMR CNRS 8108 5 Bd Descartes, 77454 Marne-la-Vallée cedex 2, France* (4) *Department of Physics, Trinity College, Dublin 2, Republic of Ireland*

The elegant properties of conformal mappings, when applied to two dimensional (2D) lattices, find interesting applications in 2D foams and other cellular or close packed structures. In particular the 2D honeycomb (whose dual is the triangular lattice) may be transformed into various conformal patterns, which compare approximately to experimentally realisable 2D foams. We review and extend the mathematical analysis of such transformations, with several illustrative examples. New results are adduced for the local curvature generated by the transformation.

Keywords: Conformal Crystals, Foams, Curvature

1. Introduction

The relationship $w = f(z)$, where f is any analytical function, can be viewed as a mapping which sets up a correspondence between the points of the z and w planes. Such mappings are known as conformal mappings. The geometrical operations of inversion, reflection, translation and magnification are all examples of conformal transformations in Euclidean space. Conformal mappings have a number of interesting properties, the most important being isogonality: any two curves that intersect are transformed into curves that intersect *at the same angle*.

Consider a discrete 2D set of points in the z -plane generated by two primitive vectors: the resulting structure in the image plane, due to a conformal mapping, is known as a *conformal lattice*. It is therefore a purely geometrical object. A *strictly conformal crystal* is a physical system consisting of particles located on the sites of a conformal lattice. A *conformal crystal* is a physical system, in which the arrangement of particles approximates a conformal lattice, see Rothen and Pierański (1996).

There are numerous examples of conformal crystals occurring both in nature and in the laboratory; see for example Rothen et al (1993, 1996), despite this the geometric properties of conformal crystals are at present poorly understood. In the present paper we examine some of the factors which determine the local curvature in these conformal patterns. We shall begin our analysis by considering the equation for the complex curvature, which was derived by by Needham (1997) and also by Mancini and Oguey (2005 a,b). For a given line in the z -plane, we shall see that whereas the first derivative of the transforming function relates the direction of a line to its transformed counterpart, the induced curvature involves the second

derivative. Here we shall use the equation for the induced curvature to compute the mean and mean square curvature of the conformal lattice

One of the most easily recognised examples of a naturally occurring conformal crystal is the phyllotactic design of a sunflower, see Rothen et. al. (1993). Another example is the so called “gravity’s rainbow” structure, which is the name given to the striking arrangement of arches formed by a cluster of magnetised steel balls in an external force field, see Rothen et. al. (1993). More recently, conformal lattices have been shown to have a connection with disclinations in 2D crystalline structures, see Mughal and Moore (2007) and Riviera et. al. (2005).

Conformal crystals can be physically realised by sandwiching an ordered, quasi 2D, foam in a Hele-Shaw cell with non-parallel plates, see for example Drenckhan et. al. (2004). Yet another method involves the use of ferrofluid foams in magnetic fields, see Elias et. al.(1999). The advantage of these foam-based methods is that a variety of conformal crystals can be realised by tuning the geometry of the experiment. However, the use of foams to approximate conformal lattices involves two complications: firstly as was shown by Mancini and Oguey (2005 a, b) the curvature of the soap films *perpendicular* to the glass plates has to be taken into account, secondly the total curvature of a soap film must always be constant. The limitations that these conditions impose on realising a given conformal crystal, using foams, will be discussed in detail below.

The paper is organised as follows. In section 2 we introduce the complex curvature and give some properties of conformal transformations. The relationship between ordered 2D soap froths and conformal transformations is detailed in section 3. In section 4 we calculate the mean curvature and the mean square curvature of the conformal lattice when the original lattice in the z-plane is free of curvature. We illustrate these results with some examples which include the case of complex inversion. In section 5 we generalise our results and include the case where the original lattice in the z-plane has a curvature. In section 6 we compute the higher order terms in the expression for the complex curvature.

2. Some Properties of Conformal Transformations

(a) *Scaling of Areas*

Although a conformal mapping $w = f(z)$ preserves angles (the isogonal property) it does not preserve areas. If $ds_z = (dx^2 + dy^2)^{\frac{1}{2}}$ is a small element of line in the (x,y) plane, upon being mapped to the w-plane it will be magnified and have a length given by,

$$ds_w = \left| \frac{dw}{dz} \right| ds_z = |f_1(z)| ds_z, \quad (2.1)$$

where $f_n(z)$ is the nth derivative of the function $f(z)$. Hence a small element of area in the z plane, denoted by dA_z , will upon being mapped to the w-plane have an area

$$dA_w = \left| \frac{dw}{dz} \right|^2 dA_z = |f_1(z)|^2 dA_z. \quad (2.2)$$

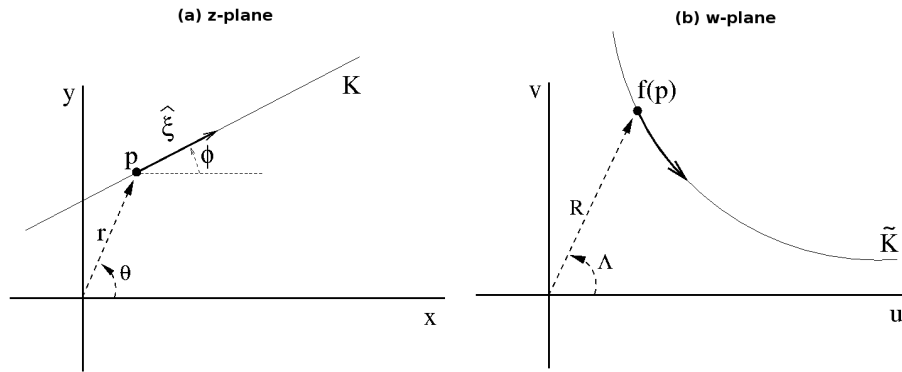


Figure 1. **(a)** For simplicity we choose to consider a straight line K , in the z -plane, which has no curvature (i.e. $\kappa = 0$). As shown the tangent vector $\xi(\phi)$ at the point p makes an angle of ϕ with the x axis. **(b)** In the image plane the effect of the analytical mapping is to yield a curve \tilde{K} , the curvature of which is given by $\tilde{\kappa}$. After Needham (1997)

(b) Complex Curvature

Consider a curve K in the z -plane: if we apply an analytical mapping f to this curve then it will transform into another curve in the image plane, which we denote by \tilde{K} . Let us now choose some arbitrary point on K which we denote by $p = x + iy = re^{i\theta}$. The unit tangent vector to the curve at point p is given by $\xi(\phi) = e^{i\phi}$, where ϕ is the angle the tangent vector makes with the x axis; for an illustration see Fig. (1a). Upon applying an analytical transformation, point p is mapped to a new point in the image plane which has coordinates $f(p) = u + iv = Re^{i\Lambda}$. It has been shown, see Needham (1997), that if the instantaneous curvature of K at the point p is given by κ , then the instantaneous curvature at $f(p)$ is given by,

$$\tilde{\kappa} = \frac{1}{|f_1(p)|} \text{Im} \left[\frac{f_2(p)}{f_1(p)} \widehat{\xi(\phi)} \right] + \frac{\kappa}{|f_1(p)|}, \quad (2.3)$$

where Im is the imaginary component, see Fig.(1b). The first term in Eq. (2.3) is the curvature in the image plane if K is a straight line. If however K has a curvature κ , then in the image plane this additional curvature is scaled by a factor of $1/|f_1(p)|$; again see Needham (1997) for a beautiful derivation of these and other results.

The utility of Eq. (2.3) can be demonstrated by a short example. Consider the mapping,

$$w = f(z) = z^\alpha, \quad (2.4)$$

where

$$f_1(z) = \alpha z^{\alpha-1} \quad \text{and} \quad f_2(z) = \alpha(\alpha-1)z^{\alpha-2}, \quad (2.5)$$

and let us represent the z -plane and the image plane in terms of complex polar coordinates so that,

$$z = re^{i\theta} \quad \text{and} \quad w = Re^{i\Lambda}.$$

Upon substituting Eq. (2.5) into Eq. (2.3), we find that the the effect of mapping a straight line in the z -plane (i.e. $\kappa = 0$) is to yield a curve in the w -plane with

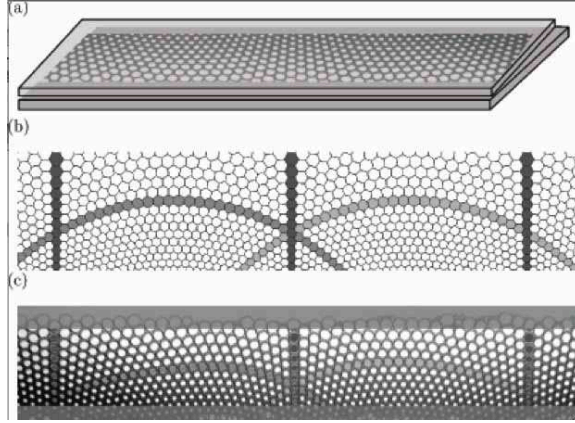


Figure 2. From Drenckhan et. al. (2004): a realisation of the logarithmic map (also known as the gravity's rainbow structure). **(a)** Experimental setup. Monodisperse bubbles are trapped between two glass plates, the lower plate is horizontal while the upper plate is angled. This arrangement induces specific variation of the bubble area with position in the foam. **(b)** Numerical mapping of the perfect honeycomb using the transformation $w = (i\alpha)^{-1} \log(i\alpha z)$. **(c)** Experimentally obtained pattern. The shading shows how lines that were initially straight are transformed.

curvature,

$$\tilde{\kappa} = \frac{1}{\alpha r^{\alpha-1}} \text{Im} \left[\frac{\alpha-1}{z} \widehat{\xi(\phi)} \right].$$

Writing out $\widehat{\xi(\phi)}$ explicitly and simplifying, this becomes,

$$\tilde{\kappa} = \frac{1}{\alpha r^{\alpha-1}} \text{Im} \left[\frac{\alpha-1}{r e^{i\theta}} (e^{i\phi}) \right] = \frac{\alpha-1}{\alpha} \frac{1}{r^{\alpha-1}} \text{Im} \left[\frac{e^{i(\phi-\theta)}}{r} \right] = \frac{\alpha-1}{\alpha} \frac{1}{r^\alpha} \sin(\phi-\theta).$$

Note, the curvature is expressed in terms of the coordinates of the z-plane. To get the curvature in the w-plane we must use the relationship $R = r^\alpha$, which gives

$$\tilde{\kappa} = \frac{\alpha-1}{\alpha} \frac{1}{R} \sin(\phi-\theta).$$

Thus the maximum curvature occurs when the tangent vector is perpendicular to the vector connecting the origin to the point p and is given by,

$$|\tilde{\kappa}_{max}| = \frac{\alpha-1}{\alpha} \frac{1}{R}. \quad (2.6)$$

This means that lines, in the z-plane, drawn perpendicular to the vector connecting the origin with point p will acquire the greatest curvature, while lines drawn parallel to it will not suffer any curvature.

3. Properties of 2D Soap Foams and Their Relationship to Conformal Transformations

A dry 2D foam consists of 2D bubbles separated by lines which meet at vertices. Such a foam can be represented by a network consisting of 2D cells separated by

1D edges. Equilibrium conditions impose strict restrictions on the topology and geometry of such a foam network (see Weaire and Hutzler (2001)): Plateau's law stipulates that the edges can intersect only three at a time and must do so at an angle of $2\pi/3$; the edges themselves have a constant curvature (circular arcs) and the curvature is related to the corresponding pressure difference between the adjacent bubbles by the Laplace-Young relation. It follows that the sum of the curvatures of the three edges at a given vertex vanishes, or equivalently that the mean curvature of the adjoining edges vanishes.

All of the above conditions are automatically satisfied by complex inversion, $f(z) = 1/z$, or more generally a bilinear conformal transformation which has the form

$$f(z) = \frac{az + b}{cz + d}.$$

It can be decomposed into four sequential transformations: translation, inversion, expansion and rotation, and a final translation, see Needham (1997). Of these only inversion is non-trivial. Conformality ensures that the mean curvature at each vertex vanishes, while only complex inversion (or a bilinear transformation) has the special property that it will map a circular arc into another circular arc. Given a dry 2D foam structure at equilibrium, inversion will therefore produce a new equilibrium structure; this was discussed by Weaire (1999) who used it to provide a neat proof of the Decoration Theorem.

A quasi 2D foam can be realised by sandwiching a single layer of bubbles between a pair of narrowly separated glass plates (Hele-Shaw cell). In the ideal case, if all the bubbles trapped in the Hele-Shaw cell have the same volume (monodisperse), then an ordered quasi 2D foam can be realised. Upon viewing the Hele-Shaw cell from above (i.e. from the direction perpendicular to the plates) the bubbles are observed to form a honeycomb structure.

Let us now assume that the bottom plate of the Hele-Shaw cell is flat while the upper plate is slightly angled or curved, if the bubbles are monodisperse, then this imposes a specific variation in the area of the bubbles. The variation in the bubble area can be made to closely match the variation required by a given conformal transformation - as stipulated by Eq. (2.2). Note that although the area of the bubbles (as observed from the direction perpendicular to the bottom plate) may change their volume remains constant, thus the height of the upper surface is related to the analytical function $f(z)$ by $h(w) = 1/dA_w$. This fact has been used to transform the (straight-edged) honeycomb structure, in a variety of ways, to generate approximations of conformal lattices (i.e. conformal crystals) Drenckhan (2004), see for example Fig. (2).

In the case of a quasi 2D foam it is important to remember that the boundaries between bubbles are in fact 2D soap films and not 1D edges, as they are often approximated. Thus, as noted by Mancini and Oguey (2005 a,b), the mean curvature of the soap film H is the average of the transverse curvature κ_t (i.e. the curvature of soap film in the direction perpendicular to the glass plates) and longitudinal curvature κ (i.e. the curvature parallel to the glass plates),

$$H = \frac{1}{2}(\kappa + \kappa_t).$$

Mancini and Oguey considered two cases. The first is the trivial case when the internal pressure is the same for all bubbles in the conformal crystal and thus $\kappa_t = -\kappa$ and $H = 0$. From an experimental perspective this case is somewhat artificial. Of more direct relevance to experimental situations is the second case where the volume of all the bubbles is the same. In this case it is found that $\kappa_t = -2\kappa$ and therefore that the mean curvature does not vanish and is given by $H = -\frac{1}{2}\kappa$.

Since in the case of constant volume bubbles, in general the longitudinal curvature κ - and therefore the mean curvature H - is not constant for a given arc it is important to know by how much the total curvature deviates from being a constant (as required by the conditions of equilibrium). This discrepancy sets a limit on the applicability of conformal transformations in the context of foams. In section VI we calculate the magnitude of this discrepancy to lowest order.

4. Lattice Curvature and Conformal Transformations

In this section we shall examine the curvature that a lattice, in the z -plane, acquires upon being mapped to the w -plane. Although the triangular lattice is of primary importance, the results derived are general enough to include other structures. This includes the square lattice and the honeycomb structure. To keep things simple we only consider the case where the original edges in the z -plane, connected to a given vertex, are free of curvature. This condition will be relaxed in the next section.

Consider a vertex in the z -plane located at $p=x+iy$. Connected to this vertex $m \geq 3$ straight edges labelled ξ_n , with $n = 0, 1, 2, \dots, m$, see Fig. (3). The angular separation between the tangent vectors of successive edges being equal to $2\pi/m$. In the case of $m = 6$ or $m = 4$ it is possible to define two edges, which are connected to the vertex, as primitive vectors and thus tessellate the z -plane forming a triangular or square Bravais lattice, respectively. We cannot, however, generate the honeycomb structure in the same way (using a vertex with $n = 3$) since the honeycomb structure is not a Bravais lattice. Nevertheless we can tessellate the z -plane with a honeycomb structure, in a unique way, by making a Voronoi construction of the points which define a triangular lattice. This is because the triangular lattice and the honeycomb structure together define a Voronoi/Delaunay dual.

In each case the tessellation in the z -plane can be thought of as consisting a vertex to which they are connected a number of straight edges of finite length. In the following we shall examine the effect a conformal mapping has on these edges. We shall compute their curvature in the image plane - from which we can compute the mean and mean square curvature of the edges connected to a given vertex in the image plane.

(a) *The Complex Curvature of an Edge Upon Being Mapped to the Image Plane*

Upon applying an analytical mapping, the vertex will now be located at a point $f(p)=u+iv$ in the w -plane. Since all the edges are straight, using Eq. (2.3) it is found that the m edges have a new curvature in the image plane given by,

$$\widehat{\kappa}_n = \frac{1}{|f_1(p)|} \text{Im} \left[\frac{f_2(p)}{f_1(p)} \widehat{\xi}_n \right] = \frac{|f_2(p)|}{|f_1(p)|^2} \text{Im} \left[e^{i\Theta} \widehat{\xi}_n \right], \quad (4.1)$$

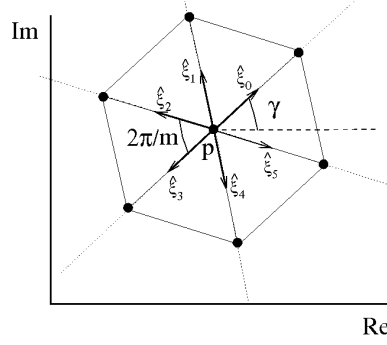


Figure 3. Consider a vertex located at point p in the z -plane, connected to which there are m straight edges. From the point p we can draw tangent vectors along each edge which is denoted by $\widehat{\xi}_0, \widehat{\xi}_1, \dots, \widehat{\xi}_{m-1}$. The angular separation between the tangent vectors is given by $2\pi/m$. We define an angle γ which is the angle between the x -axis and the first vector $\widehat{\xi}_0$. Thus the angle that the n th vector makes with the x axis is $2\pi n/m + \gamma$. Clearly the edges are invariant under a rotation of $2\pi/m$ and so we restrict γ to the range $0 \leq \gamma < 2\pi/m$.

where we have set (i.e. $\kappa_n = 0$ i.e. the curvature of the edges in the z plane). We also have

$$\Theta = \theta_2 - \theta_1 = \text{Arg} \left[\frac{f_2(p)}{f_1(p)} \right],$$

and Arg stands for the complex argument. From here on we shall adopt the notation that

$$\theta_n = \text{Arg}[f_n(p)].$$

The n th tangent vector is given by,

$$\widehat{\xi}_n = e^{i(\frac{2\pi n}{m} + \gamma)},$$

where γ is the angle made by the 0th tangent vector, in the z -plane, with the x axis. This is shown schematically in Fig. (3). Eq. (4.1) can be written as,

$$\widetilde{\kappa}_n = \frac{|f_2(p)|}{|f_1(p)|^2} \sin \left(\Theta + \frac{2\pi n}{m} + \gamma \right) = \frac{|f_2(p)|}{|f_1(p)|^2} \sin \left(s + \frac{2\pi n}{m} \right), \quad (4.2)$$

where $s = \gamma + \Theta$.

(b) *The Mean Complex Curvature of the Edges, Connected to a Given Vertex, in the Image Plane*

Let us define the mean curvature of the edges in the z -plane as,

$$C_m = \frac{1}{m} \sum_{n=0}^{n=m-1} \kappa_n,$$

similarly, the mean curvature of the edges in the w -plane as,

$$\widetilde{C}_m = \frac{1}{m} \sum_{n=0}^{n=m-1} \widetilde{\kappa}_n = \frac{1}{m} \frac{|f_2(p)|}{|f_1(p)|^2} \sum_{n=0}^{n=m-1} \sin \left(s + \frac{2\pi n}{m} \right) = 0, \quad (4.3)$$

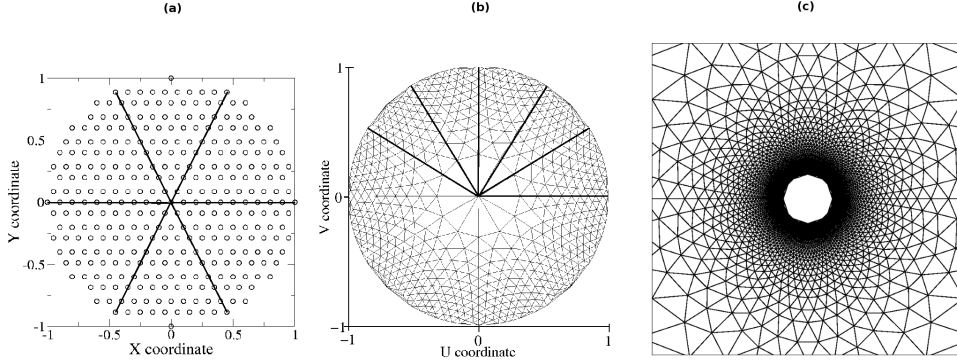


Figure 4. **(a)**: a circular disk cut out of a triangular lattice in the z plane, where the angle between each successive heavy line is $\pi/3$. Clearly the lattice lines are free of curvature. Upon applying a conformal transformation, **(b)**: $w = z^{1/2}$ and **(c)**: complex inversion, i.e. $w = 1/z$, the result is a conformal lattice in the image plane. Note that in the case of $w = z^{1/2}$ the conformal lattice has been produced by allowing the range of the z plane to extend to $\phi < 4\pi$. In both cases the mean curvature vanishes everywhere but the mean square curvature does not. Also the mean square curvature diverges at the origin, which for both transformations is a critical point. At the critical point the angle preserving property of the transformation breaks down, this can be easily seen in the case of the $w = z^{1/2}$ transformation - instead of being preserved, the angle $\pi/3$ between rays (heavy lines) emanating from the origin is halved.

where we have substituted Eq. (4.2) into Eq. (4.3). This result is rather trivial it merely expresses the fact that in the image plane, connected to each vertex, there are pairs of opposed edges for which the sum of their curvatures always vanish.

(c) *The Mean Square Value of the Complex Curvature of the Edges, Connected to a Given Vertex, in the Image Plane*

Since the mean curvature always vanishes, the mean square curvature of the edges in the z -plane is simply defined as,

$$Q_m = \frac{1}{m} \sum_{n=0}^{n=m-1} k_n^2, \quad (4.4)$$

and in the w -plane the mean square curvature is,

$$\widetilde{Q}_m = \frac{1}{m} \sum_{n=0}^{n=m-1} \widetilde{k}_n^2 = \frac{1}{m} \left(\frac{|f_2(p)|}{|f_1(p)|^2} \right)^2 \sum_{n=0}^{n=m-1} \sin^2 \left(s + \frac{2\pi n}{m} \right) = \frac{1}{2} \left(\frac{|f_2(p)|}{|f_1(p)|^2} \right)^2. \quad (4.5)$$

where we have substituted Eq. (4.2) into Eq. (4.5). Thus the mean square curvature of the edges, connected to a given vertex in the image plane, is independent with respect to the orientation of the vertex in the image or z planes.

(d) *Examples*

To illustrate the results derived for the mean and mean square curvature, we now examine two conformal lattices which have been generated by applying a trans-

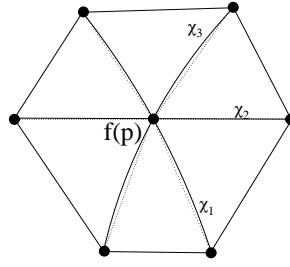


Figure 5. This diagram shows the effect of the transformation $f(z)$ on a hexagonal lattice cell, which in the z plane has its centre at p . In the w -plane the lattice cell becomes deformed and its centre is now to be found at $f(p)$. The deformed hexagonal cell can be decomposed into three arcs which cross the centre of the cell. Each arc can in turn be decomposed into points, to which we fit the equation of a circle. From this it is possible to calculate the curvature of each arc, represented here by χ_1 , χ_2 and χ_3 .

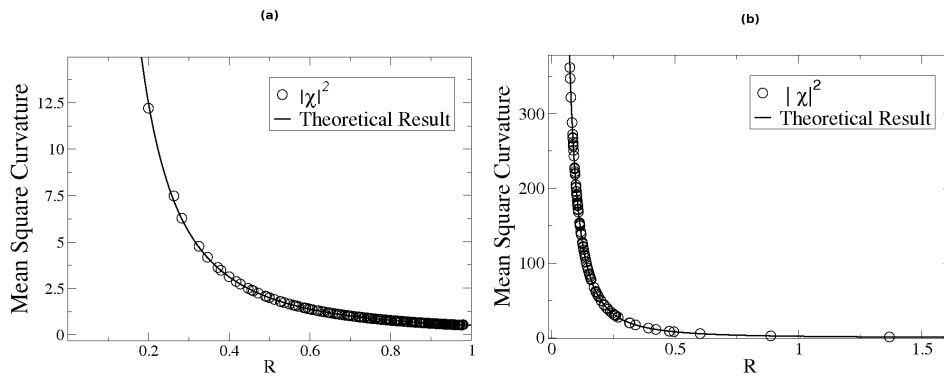


Figure 6. Mean square curvature for the mapping **(a)** $f(z) = z^{1/2}$ and **(b)** $f(z) = 1/z$.

formation to a circular disk cut out of a triangular lattice. Just such a cut out is shown in Fig.(4a), it can be seen that the lattice is free of curvature. Applying the mapping $f(z) = z^{1/2}$ to the triangular lattice in the z -plane yields a conformal lattice in the image plane, see Fig.(4b). From Eq. (4.5) the mean square curvature is found to be

$$\widetilde{Q}_m = \frac{1}{2r} = \frac{1}{2R^2}, \quad (4.6)$$

where we have transformed from the coordinates in the z -plane (r, λ) to the w -plane coordinates (R, Λ) . Similarly, the effect of inversion is shown in the bottom part of Fig.(4). To compute the mean square curvature we substitute $f(z) = 1/z$ into Eq. (4.5), which yields,

$$\widetilde{Q}_m = \frac{r^2}{2} = \frac{2}{R^2}. \quad (4.7)$$

To verify our results we estimate the mean square curvature directly from the transformed lattice. To do so, note that any given hexagonal cell in the image plane can be decomposed into three arcs which cross the the centre of the cell at $f(p)$, as shown in Fig. (5). Each of these three arcs can be further decomposed into three

points which can be used to fit the equation of a circle, from which the curvature of the arc can be readily computed. Let us denote the three directly computed curvatures as χ_1, χ_2 and χ_3 . We can define the mean square curvature as,

$$|\chi|^2 = \frac{1}{3}(\chi_1^2 + \chi_2^2 + \chi_3^2). \quad (4.8)$$

Thus, for the two conformal lattices shown in fig 4, we can estimate the mean square curvature for a given vertex using Eq. (4.8). The results are shown by the circles in Fig. (6) along with the theoretical results Eq. (4.6) and Eq. (4.7).

Except in the case of complex inversion there will be a difference between the analytical value of the curvature and the estimated curvature. This is due to the fact that the curves to which we have fitted the circles are not themselves circular arcs. We quantify this discrepancy in section VI of this paper.

5. Some Generalisations

In the previous section we considered a vertex, in the z-plane, to which there are connected a finite number of straight edges. We found that when the vertex is mapped to the image plane the mean curvature of the edges vanishes and that the mean square curvature is independent with respect to the orientation of the vertex.

Let us now consider the case where the edges connected to a vertex, in the z-plane, have some initial curvature. Let us also assume that the number of edges connected to the vertex is infinite. As the number of edges tends to infinity, the tangent vectors together describe a circle of unit radius centred on the vertex. Upon averaging over the length of the circle the mean curvature of the edges in the z-plane can be written as,

$$C = \frac{1}{2\pi} \int_0^{2\pi} \kappa(\phi) d\phi, \quad (5.1)$$

where $\kappa(\phi)$ is now a continuous function over the range $0 \leq \phi < 2\pi$ and describes the curvature of the edges in the z-plane. Similarly, the mean curvature of the edges upon being transformed to the w-plane is given by,

$$\tilde{C} = \frac{1}{2\pi} \int_0^{2\pi} \widetilde{\kappa(\phi)} d\phi. \quad (5.2)$$

where we define,

$$\widetilde{\kappa(\phi)} = \frac{1}{|f_1(p)|} \text{Im} \left[\frac{f_2(p)}{f_1(p)} \widehat{\xi(\phi)} \right] + \frac{\kappa(\phi)}{|f_1(p)|}, \quad (5.3)$$

Eq. (5.3) can be written as

$$\widetilde{\kappa(\phi)} = \frac{1}{|f_1(p)|} \text{Im} \left[T e^{i\Theta} \widehat{\xi(\phi)} \right] + \frac{\kappa(\phi)}{|f_1(p)|} = \frac{|f_2(p)|}{|f_1(p)|^2} \text{Im} \left[e^{i\Theta} \widehat{\xi(\phi)} \right] + \frac{\kappa(\phi)}{|f_1(p)|},$$

where T and Θ have the same definitions as in section IV. Writing out $\widehat{\xi(\phi)}$ explicitly and simplifying gives

$$\widetilde{\kappa(\phi)} = \frac{|f_2(p)|}{|f_1(p)|^2} \sin(\Theta + \phi) + \frac{\kappa(\phi)}{|f_1(p)|}. \quad (5.4)$$

Substituting Eq. (5.4) into Eq. (5.2) yields,

$$\tilde{C} = \frac{1}{2\pi} \frac{|f_2(p)|}{|f_1(p)|^2} \int_0^{2\pi} \sin(\Theta + \phi) d\phi + \frac{C}{|f_1(p)|} = \frac{C}{|f_1(p)|}. \quad (5.5)$$

Thus the conformal transformation scales the original mean curvature by the magnification factor $1/|f_1(p)|$ of the transformation (see Eq. (2.1)).

Since the mean curvature does not necessarily vanish, we define the mean square curvature in the z-plane as,

$$Q = \frac{1}{2\pi} \int_0^{2\pi} (\kappa(\phi) - C)^2 d\phi, \quad (5.6)$$

similarly we define the mean square curvature in the w-plane as,

$$\tilde{Q} = \frac{1}{2\pi} \int_0^{2\pi} (\widetilde{\kappa(\phi)} - \tilde{C})^2 d\phi = \frac{1}{2\pi} \int_0^{2\pi} (\widetilde{\kappa(\phi)}^2 - 2\tilde{C}\widetilde{\kappa(\phi)} + \tilde{C}^2) d\phi, \quad (5.7)$$

substituting Eq. (5.4) into Eq. (5.7) and performing the resulting integrals gives,

$$\tilde{Q} = \frac{1}{2} \left(\frac{|f_2(p)|}{|f_1(p)|^2} \right)^2 + \frac{Q}{|f_1(p)|^2} + \frac{1}{\pi} \frac{|f_2(p)|}{|f_1(p)|^3} \int_0^{2\pi} \kappa(\phi) \sin(\Theta + \phi) d\phi. \quad (5.8)$$

The first term is the mean square curvature of the edges in the image plane if the edges in the z-plane have no curvature. The second term simply states that the original mean square curvature of the edges is scaled by a factor of $1/|f_1(p)|^2$. The third term is a coupling between the original curvature of the edges and the transformation $f(z)$. To get a better understanding of the third term let us label it as \tilde{Q}_3 . It can be written as,

$$\tilde{Q}_3 = \frac{1}{\pi} \frac{|f_2(p)|}{|f_1(p)|^3} \int_0^{2\pi} \kappa(\phi) (\sin \Theta \cos \phi + \cos \Theta \sin \phi) d\phi. \quad (5.9)$$

Since $\kappa(\phi)$ is an arbitrary function which exists over the interval $0 \leq \phi < 2\pi$, it is natural to express it in terms of a Fourier series, so that,

$$\kappa(\phi) = \frac{1}{2} a_0 + \sum_{q=1}^{\infty} a_q \cos(q\phi) + b_q \sin(q\phi). \quad (5.10)$$

Substituting Eq. (5.10) into Eq. (5.9) we find,

$$\tilde{Q}_3 = \frac{|f_2(p)|}{|f_1(p)|^3} (a_1 \sin \Theta + b_1 \cos \Theta), \quad (5.11)$$

thus the only contribution to the mean square curvature is from the mode $q = 1$. The contributions from all other modes cancel out, so that an increase in mean square curvature for a given edge is cancelled out by a decrease in mean square curvature for some other edge. Furthermore Eq. (5.11) depends on the orientation of the vertex in the z-plane through the angle Θ . The turning points (i.e. the the maximum and minimum mean square curvature) depend on the values of the coefficients a_1 and b_1 and are located at $\Theta = \tan^{-1}(a_1/b_1)$ and $\Theta = \tan^{-1}(a_1/b_1) + \pi$.

Thus when the edges in the z-plane are not free of curvature the effect of the conformal mapping is to scale the mean curvature, while the mean square curvature is found to be no longer independent with respect to orientation of the vertex.

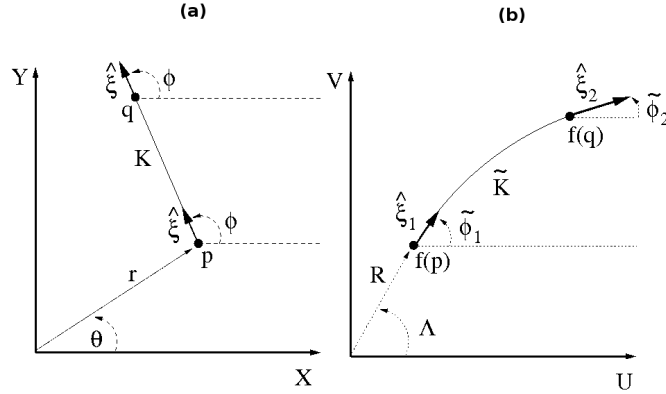


Figure 7. (a) This diagram shows a straight line K in the z -plane. The line starts at the point labelled p and ends at q , it has a total length L . At both points the unit tangent vector has the same direction and makes an angle of ϕ with the x -axis. (b) This diagram shows the resulting curve \tilde{K} in the image plane due to the conformal mapping $w = f(z)$. The curve begins at the point labelled $f(p)$ and ends at $f(q)$ and now has a length \tilde{l} . In general the angle that the tangent vectors make at $f(p)$ and $f(q)$, which are labelled $\tilde{\phi}_1$ and $\tilde{\phi}_2$ respectively, will no longer be equal.

6. Higher Order Terms in the Complex Curvature

For a given 2D plane curve its curvature is defined as the rate of change of the angle of the tangent vector with respect to the distance along the curve. We can think of this as limiting process: take two tangent vectors a short distance apart on the curve, measure the angle they make with respect to a fixed axis, and take the limit in which the separation between the tangent vectors vanishes. This then gives the instantaneous value of the curvature.

Consider a 2D plane curve in the image plane which has been generated by applying a complex mapping to some curve in the z plane. We can choose a pair of points on the image curve a *finite* distance apart and for both points construct a tangent vector. Thus we can ask: what is the rule which gives the total difference in angle between the two tangent vectors?

In this section we derive an expression for the *average complex curvature* which we define as: the total change in the angle of the tangent vector over a segment of a curve averaged over the length of the segment. The result is a series expansion in which Eq. (2.3) is the lowest order term. This series expansion will lead us to an expression which can be used to measure the degree to which a given image arc differs from being perfectly circular. Here we shall only consider the effect of the mapping $w = f(z)$ on a straight line in the z -plane. Furthermore, we shall assume that the effect of the mapping is to produce a open, simple and well behaved curve in the image plane.

Consider a straight line K in the z plane, which joins point p to q and let us assume it has a length $|\xi|$. This is shown in Fig. (7a). At p we have drawn the unit tangent vector $\hat{\xi} = e^{i\phi}$, so that the vector joining p to q is given by

$$\xi = |\xi| \widehat{\xi(\phi)}. \quad (6.1)$$

The line K is described by the equation

$$K = z(t) = p + t\widehat{\xi} = re^{i\theta} + te^{i\phi}, \quad (6.2)$$

where $0 \leq t \leq |\xi|$. Note that at $t = 0$ we have $z = p$ and at $t = |\xi|$ we have

$$z(|\xi|) = q = p + \xi = re^{i\theta} + |\xi|e^{i\phi}.$$

Thus K has been parametrised by the free parameter t which measures the distance along K from the point p . The line K has a real component and imaginary components

$$x(t) = r \cos \theta + t \cos \phi \quad \text{and} \quad y(t) = r \sin \theta + t \sin \phi.$$

respectively.

Now consider what happens if we apply an analytical mapping $w = f(z)$ to K , the result is a new curve \widetilde{K} in the image plane which starts at the point labelled $f(p)$ and ends at $f(q)$ - as shown in Fig. (7b). This curve now has some new length which we call l (not to be confused with the chord distance between $f(p)$ and $f(q)$). We define the *average* complex curvature of the image curve \widetilde{K} as

$$\widetilde{\mathbb{K}} = \frac{\Delta\widetilde{\phi}}{l} = \frac{\widetilde{\phi}_2 - \widetilde{\phi}_1}{l}. \quad (6.3)$$

where the tangent vectors at $f(p)$ and $f(q)$ are labelled $\widehat{\xi}_1$ and $\widehat{\xi}_2$ and make an angle of $\widetilde{\phi}_1$ and $\widetilde{\phi}_2$, respectively, with the u axis.

If for Eq. (6.3) we keep the point p fixed and take the limit in which $|\xi|$ goes to zero we recover the instantaneous curvature of the curve \widetilde{K} at the point $f(p)$, that is

$$\widetilde{\kappa}(p) = \lim_{|\xi| \rightarrow 0} \widetilde{\mathbb{K}},$$

Let us now define the difference between the instantaneous curvature of the image arc at its starting point and the average curvature of the arc, which we denote as

$$\Delta\widetilde{\mathbb{K}} = \widetilde{\mathbb{K}} - \widetilde{\kappa}(p).$$

We note that if the image arc is a perfect circle then the instantaneous curvature has a constant value at every point on the arc and therefore $|\Delta\widetilde{\mathbb{K}}| = 0$. This fact can be used to quantify the degree to which the image curve deviates from perfect circularity.

In the context of 2D and quasi 2D foams it is important to know the degree to which a given arc, generated by a conformal mapping, deviates from perfect circularity. Laplace's law requires that the curvature of a soap film is constant, therefore for a 2D soap film a large value of $|\Delta\widetilde{\mathbb{K}}|$ implies a large error in how well the soap film approximates the conformal lattice. The same holds true for quasi 2D foams (in the constant volume regime), except that we have to remember that the total curvature of the soap film, i.e. the sum of longitudinal ($\kappa = \kappa(p)$) and transverse (κ_t) curvatures, has an instantaneous value of

$$H = -\frac{1}{2}\widetilde{\kappa}(p).$$

In either case Laplace's law is satisfied only if the soap film has a constant longitudinal curvature, i.e. it describes a circular arc when viewed from a direction perpendicular to the bottom plate of the Hele-Shaw cell.

In the following we shall decompose the task of finding $\tilde{\mathbb{K}}$ into two parts: firstly we compute l and secondly we compute $\Delta\tilde{\phi}$.

(a) *Arc Length in the Image Plane*

As stated above: the real and imaginary components of the line \mathbb{K} are a function of the free parameter t . Upon mapping \mathbb{K} to the image plane, (using the analytical function $w = f(z)$) the result is the image curve $\tilde{\mathbb{K}}$ - the real and imaginary components of which are also functions of the free parameter t and denoted by $u(t)$ and $v(t)$, respectively. We can write the real and imaginary components of $\tilde{\mathbb{K}}$ in the form of a series expansion about the point p (i.e. $t = 0$), giving

$$u(t) = u + t \frac{u_t}{1!} + t^2 \frac{u_{tt}}{2!} + \dots + \text{h.o.t.} \quad (6.4)$$

and also

$$v(t) = v + t \frac{v_t}{1!} + t^2 \frac{v_{tt}}{2!} + \dots + \text{h.o.t.} \quad (6.5)$$

where,

$$u = u(t)|_{t=0} = u(0) \quad (6.6)$$

$$u_t = \left. \frac{du(t)}{dt} \right|_{t=0} \quad (6.7)$$

$$u_{tt} = \left. \frac{d^2u(t)}{dt^2} \right|_{t=0} \quad (6.8)$$

and so on. We also define v_t and v_{tt} (and higher order terms) in a similar manner.

The total length of the arc $\tilde{\mathbb{K}}$ is given by,

$$l = \int_0^{|\xi|} \sqrt{\left(\frac{du(t)}{dt}\right)^2 + \left(\frac{dv(t)}{dt}\right)^2} dt. \quad (6.9)$$

We can substitute Eq.(6.4) and Eq.(6.5) into Eq.(6.9), then expand the integrand in powers of t , and integrate each term with respect to t to give,

$$l = l_0|\xi| + l_1|\xi|^2 + l_2|\xi|^3 \dots + \text{h.o.t.} \quad (6.10)$$

where we assume that $|\xi|$ is small enough to guarantee convergence of the series. The coefficients in Eq.(6.10) are defined as

$$l_0 = \sqrt{u_t^2 + v_t^2} \quad (6.11)$$

$$l_1 = \frac{1}{2} \frac{u_t u_{tt} + v_t v_{tt}}{\sqrt{u_t^2 + v_t^2}} \quad (6.12)$$

$$l_2 = \frac{1}{6} \sqrt{u_t^2 + v_t^2} \left[\frac{u_{tt}^2 + u_t u_{ttt} + v_t v_{ttt} + v_{tt}^2}{\sqrt{u_t^2 + v_t^2}} - \frac{(u_t u_{tt} + v_t v_{tt})^2}{2(u_t^2 + v_t^2)^2} \right]. \quad (6.13)$$

We notice that the coefficients given by Eq.(6.11) to Eq.(6.13) (and higher order terms) are defined with respect to the parameter t . In order to express the coefficients in terms of the complex number z we use Eq. (6.2) from which we have the relationship $dz/dt = e^{i\phi}$, this can be rearranged to give $dt = e^{-i\phi}dz$. Thus Eq.(6.6) to Eq.(6.8) (and higher order derivatives) can be written as

$$\begin{aligned} \left. \frac{d^n u}{dt^n} \right|_{t=0} &= \operatorname{Re} \left[\left. \frac{d^n w}{dt^n} \right|_{t=0} \right] = \operatorname{Re} \left[\left. \frac{d^n w}{(e^{-i\phi} dz)^n} \right|_{z=p} \right] = \operatorname{Re} \left[\left. \frac{d^n w}{dz^n} \right|_{z=p} e^{in\phi} \right] \\ &= |f_n(p)| \operatorname{Re} \left[e^{i(\theta_n + n\phi)} \right] = |f_n(p)| \cos(\theta_n + n\phi) \end{aligned} \quad (6.14)$$

where we have made a change of variable from t to z and used the fact that at $t = 0$ we have $z = p$; also we used

$$\left. \frac{d^n w}{dz^n} \right|_{z=p} = |f_n(z)| e^{i \operatorname{Arg}[f_n(z)]} \Big|_{z=p} = |f_n(p)| e^{i\theta_n}.$$

Similarly for the derivatives v_t and v_{tt} (and higher order terms), we have,

$$\left. \frac{d^n v}{dt^n} \right|_{t=0} = |f_n(p)| \sin(\theta_n + n\phi). \quad (6.15)$$

Finally, the coefficients given by Eq.(6.11) to Eq.(6.13) can be expressed in terms of Eq.(6.14) and Eq.(6.15) to give

$$l_0 = |f_1(p)| \quad (6.16)$$

$$l_1 = \frac{|f_1(p)|}{2} \operatorname{Re} \left[\frac{f_2(p)}{f_1(p)} \widehat{\xi(\phi)} \right] \quad (6.17)$$

$$l_2 = \frac{|f_1(p)|}{12} \left(\frac{|f_2(p)|^2}{|f_1(p)|^2} - \operatorname{Re} \left[\left(\frac{f_2(p)}{f_1(p)} \widehat{\xi(\phi)} \right)^2 - 2 \left(\frac{f_3(p)}{f_1(p)} \widehat{\xi(\phi)} \right)^2 \right] \right) \quad (6.18)$$

Upon substituting Eq.(6.16), Eq.(6.17) and Eq.(6.18) into Eq.(6.10) we have a series expansion in powers of the $|\xi|$. We note that the lowest order term in Eq.(6.10) is identical to Eq.(2.1).

(b) *Change in the angle of the tangent vector in the image plane*

We now compute the difference in angle, $\Delta\tilde{\phi} = \tilde{\phi}_2 - \tilde{\phi}_1$, of the tangent vectors in the image plane. This derivation is adapted from the one used by Needham (1997) to compute the instantaneous curvature. The difference here is that we endeavour to retain all details which may yield higher order terms in the expression for $\Delta\tilde{\phi}$.

Consider again the the straight line K in the z -plane, as shown Fig. (7). Note that the tangent vector at p upon being mapped by the function $w = f(z)$ is, after being translated to $f(p)$, magnified by a length $|f_1(p)|$ and rotated by an angle $\operatorname{Arg}[f_1(p)]$. Similarly, upon applying the mapping $w = f(z)$, the tangent vector at q is, after being translated to $f(q)$, magnified by a length $|f_1(q)|$ and rotated by an angle $\operatorname{Arg}[f_1(q)]$. However, the rotation of the tangent vector at $f(q)$ will differ very slightly by $\Delta\tilde{\phi}$ from the rotation suffered by the tangent vector at $f(p)$.

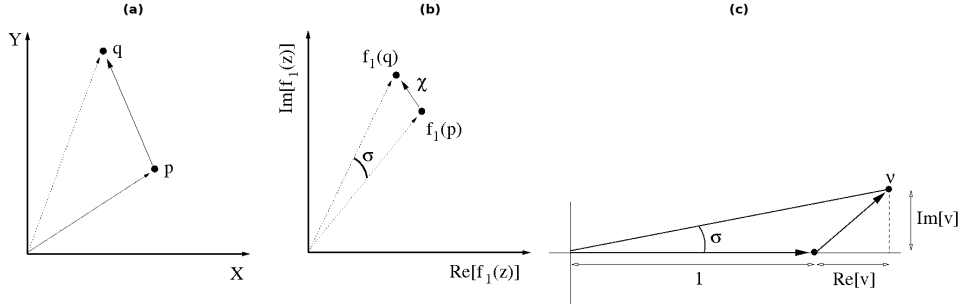


Figure 8. After Needham (1997): **(a)** This diagram shows two points p and q in the z plane. **(b)** Upon applying the mapping $f_1(z) = df(z)/dz$ the points are mapped to $f_1(p)$ and $f_1(q)$, which are connected by the vector χ . Note that to transform $f_1(p)$ into $f_1(q)$ it is necessary to magnify $f_1(p)$ by some factor and to rotate $f_1(p)$ by the angle denoted by σ . **(c)** This triangle is the result of dividing all the vectors shown in (b) by the complex number $f_1(p)$. Dividing by $f_1(p)$ has two effects: firstly the triangle is rotated so that one of its sides is now parallel to the real axis, secondly all the sides of the triangle are uniformly scaled. This second effect means that the new triangle is similar to the triangle shown (b).

To compute the difference in angle between the tangent vectors consider the two points p and q as shown in Fig. (8a), upon applying the mapping $f_1(z)$ the points are now located at $f_1(p)$ and $f_1(q)$, respectively. Where the vector connecting $f_1(p)$ to $f_1(q)$ is labelled χ and is given by

$$\chi = f_1(q) - f_1(p) = f_2(p)\hat{\xi}|\xi| + \frac{1}{2!}f_3(p)\hat{\xi}^2|\xi|^2 + \frac{1}{3!}f_4(p)\hat{\xi}^3|\xi|^3 \dots + \text{h.o.t}$$

where we have made use of Eq.(6.1).

Note, with reference to Fig. (8b), that to transform the vector $f_1(p)$ into the vector $f_1(q)$ it is necessary to expand the length of $f_1(p)$ by some factor and to rotate the vector $f_1(p)$ by an angle σ . It is this angle σ which is the extra rotation suffered by the tangent vector at $f(q)$ compared to the rotation of the tangent vector at $f(p)$, i.e. $\sigma = \Delta\tilde{\phi}$. Our task is to compute the angle σ shown on the right hand side of Fig. (8). Note, σ is part of a triangle whose sides are given by the known vectors χ , $f_1(p)$ and $f_1(q)$. To compute σ we rotate the triangle shown in Fig. (8b) to the real axis by dividing by $f_1(p)$ (this is the same trick used by Needham (1997)), the result is shown in Fig. (8c), this new triangle is geometrically similar to the original triangle shown in Fig. (8b). The side along the real axis has a length 1 and in addition the point ν is given by the vector

$$\nu = [\chi/f_1(p)]. \quad (6.19)$$

By a simple application of trigonometry we have

$$\Delta\tilde{\phi} = \sigma = \tan^{-1} \left(\frac{\text{Im}[\nu]}{1 + \text{Re}[\nu]} \right). \quad (6.20)$$

Upon substituting Eq.(6.19) into Eq.(6.20), we can expand Eq.(6.20) in powers of $|\xi|$ (we assume that $|\xi|$ is small enough to allow convergence) to give,

$$\Delta\tilde{\phi} = \sigma = \sigma_0|\xi| + \sigma_1|\xi|^2 + \sigma_2|\xi|^3 \dots + \text{h.o.t}. \quad (6.21)$$

where we have made use of Eq.(6.19), we find

$$\sigma_0 = \text{Im} \left[\frac{f_2(p)}{f_1(p)} \widehat{\xi(\phi)} \right] \quad (6.22)$$

$$\sigma_1 = \frac{1}{2} \text{Im} \left[\left(\frac{f_3(p)}{f_1(p)} - \left(\frac{f_2(p)}{f_1(p)} \right)^2 \right) \widehat{\xi(\phi)}^2 \right] \quad (6.23)$$

$$\sigma_2 = \text{Im} \left[\left(\frac{1}{3} \left(\frac{f_2(p)}{f_1(p)} \right)^3 - \frac{1}{2} \left(\frac{f_2(p)f_3(p)}{(f_1(p))^2} \right) + \frac{1}{6} \left(\frac{f_4(p)}{f_1(p)} \right) \right) \widehat{\xi(\phi)}^3 \right] \quad (6.24)$$

(c) *The Average Complex Curvature*

Substituting Eq.(6.10) and Eq.(6.21) into Eq. (6.3) and expanding in powers of $|\xi|$ yields,

$$\widetilde{\mathbb{K}} = \widetilde{\mathbb{K}}_0 + \widetilde{\mathbb{K}}_1|\xi| + \widetilde{\mathbb{K}}_2|\xi|^2 + \dots \text{h.o.t} \quad (6.25)$$

where we find,

$$\begin{aligned} \widetilde{\mathbb{K}}_0 &= \widetilde{\kappa} = \frac{1}{|f_1(p)|} \text{Im} \left[\frac{f_2(p)}{f_1(p)} \widehat{\xi(\phi)} \right] \\ \widetilde{\mathbb{K}}_1 &= \frac{1}{2|f_1(p)|} \left(\text{Im} \left[\frac{f_3(p)}{f_1(p)} \widehat{\xi(\phi)}^2 \right] - \frac{3}{2} \text{Im} \left[\left(\frac{f_2(p)}{f_1(p)} \widehat{\xi(\phi)} \right)^2 \right] \right) \\ \widetilde{\mathbb{K}}_2 &= \frac{1}{48|f_1(p)|} \left(\frac{3|f_2(p)|^2}{|f_1(p)|^2} \text{Im} \left[\frac{f_2(p)}{f_1(p)} \widehat{\xi(\phi)} \right] + 27 \text{Im} \left[\left(\frac{f_2(p)}{f_1(p)} \widehat{\xi(\phi)} \right)^3 \right] \right. \\ &\quad \left. - \frac{2|f_2(p)|^2}{|f_1(p)|^2} \text{Im} \left[\frac{f_3(p)}{f_2(p)} \widehat{\xi(\phi)} \right] - 34 \text{Im} \left[\frac{f_2(p)f_3(p)}{(f_1(p))^2} \widehat{\xi(\phi)}^3 \right] + 8 \text{Im} \left[\frac{f_4(p)}{f_1(p)} \widehat{\xi(\phi)}^3 \right] \right) \end{aligned}$$

In effect Eq.(6.25) gives the total change in the angle of the tangent vector in the image plane, as it traverses the image curve, *averaged* over the length of the curve. We observe that as $|\xi| \rightarrow 0$ then $\widetilde{\mathbb{K}} \rightarrow \widetilde{\mathbb{K}}_0 = \widetilde{\kappa}$, giving the instantaneous curvature of the image curve at the point $f(p)$.

Example $f(z) = z^3$

Let us apply Eq.(6.25) to a simple example, we choose the complex mapping $f(z) = z^3$. Consider again the a straight line in the z -plane given by Eq.(6.2), and let us set $r = 1, \theta = 0, \phi = \pi/2$ and $|\xi| = 0.1$, so that we have

$$K = z(t) = 1 + te^{i\frac{\pi}{2}}, \quad (6.26)$$

and $0 \leq t \leq 0.1$, the result is the straight line shown in Fig. (9a). Upon applying the conformal transformation $f(z) = z^3$ the result is the curve shown in Fig. (9b).

The derivatives for the function $f(z) = z^3$ are given by $f_1(z) = 3z^2, f_2(z) = 6z, f_3(z) = 6$, with all higher derivatives being equal to zero. Upon evaluating these derivatives at the point $p = re^{i\theta} = 1e^{i0} = 1$ we have $f_1(p) = 3, f_2(p) = 6$ and $f_3(p) = 6$; together with the angle of the tangent vector to the straight line at the

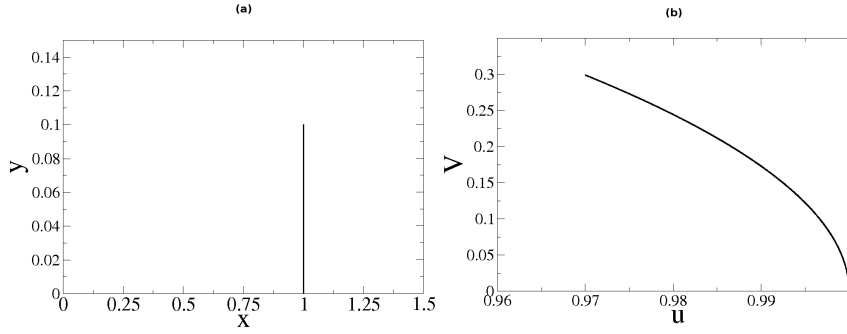


Figure 9. **(a)** A straight line in the z -plane, with $r = 1, \theta = 0, \phi = \pi/2$ and $|\xi| = 0.1$
(b) The resulting curve in the image plane generated by applying the conformal mapping $f(z) = z^3$ to the straight line defined by Eq.(6.26)

point p (i.e. $\phi = \pi/2$) and the length of the straight line in z -plane ($|\xi| = 0.1$), we find

$$\widetilde{\mathbb{K}}_0 = \frac{1}{3} \text{Im} \left[\frac{6}{3} e^{i\pi/2} \right] = \frac{2}{3} \sin \pi/2 = \frac{2}{3}$$

and similarly $\widetilde{\mathbb{K}}_1 = 0, \widetilde{\mathbb{K}}_2 = -1/2.25, \widetilde{\mathbb{K}}_3 = 0$ and $\widetilde{\mathbb{K}}_4 = 0.281481$; thus up to fourth order in $|\xi|$ we have $\widetilde{\mathbb{K}} \approx 0.66225037$.

This value can be compared to a numerically computed value. To do so, for the curve shown Fig. (9b), we need to compute the length of the curve and the total change in the angle of the tangent vector. This can be done by taking a large number of equally spaced points on the curve. By drawing a straight line between any two adjacent points we get a series of segments which approximate the curve, the approximation improves as more points are taken. It is then a simple matter for a computer to calculate the length of each segment and to find the total length of the curve by summing up the lengths of all the segments. To compute the total change in the angle of the tangent vector: we first compute the angle that the first segment makes with the u axis, then we compute the angle that the final segment makes with the u axis, by taking the difference between the two we find the change in the angle of the tangent vector between the start and the end of the curve. Upon taking 1×10^5 such equally spaced points on the curve shown in Fig. (9b) we have an numerically computed value for the average curvature, giving $\widetilde{\mathbb{K}}_{\text{Num}} = 0.6622435$. It is clear that Eq.(6.25) is converging to $\widetilde{\mathbb{K}}_{\text{Num}}$ as more terms are taken.

(d) Mean Square of the Average Complex Curvature

For the instantaneous curvature we found it useful to compute the mean square curvature, see Eq. (4.5), which is independent of the orientation of the vertex and therefore serves as a useful measure of how strongly the conformal lattice is curved at any given point in the image plane. Similarly we can compute a mean square value of the average complex curvature. We find that this leads to a series expansion in which the lowest order term is the mean square curvature given by Eq. (4.5). When the higher order terms in this expansion vanish it means that all the image edges, at that particular point in the image plane, have a constant curvature. If on

the other hand the higher order terms do not vanish this means that Laplace's law, for a 2D or quasi 2D foam used to realise the conformal lattice, cannot be perfectly satisfied for every edge. The magnitude of the higher order correction serve as an estimate of the discrepancy between the foam and the conformal map, in most practical cases the discrepancy can be assumed to be negligible if the leading order correction in the expansion is small.

Consider again a vertex p in the z -plane to which there are connected a number of straight edges of length $|\xi|$ separated by a constant angular separation, such as that shown in Fig. (3). Upon being mapped to the image plane the point p is now located at $f(p)$ and the straight edges are transformed into arcs. If we were to sum up the average complex curvature, for each of the arcs emanating from the vertex at $f(p)$, we would find that it vanishes.

If, however, for each arc we square the average complex curvature and sum up the squares we have a quantity that does not vanish. Thus we can compute the mean square value of the average complex curvature $\widetilde{\mathbb{K}}$, which we shall denote by $\widetilde{\mathbb{Q}}$, this can be done, most easily, by integrating Eq.(6.25) with respect to ϕ over the range $0 \leq \phi \leq 2\pi$ giving

$$\widetilde{\mathbb{Q}} = \frac{1}{2\pi} \int_0^{2\pi} \widetilde{\mathbb{K}(\phi)}^2 d\phi. = \widetilde{\mathbb{Q}}_0 + \widetilde{\mathbb{Q}}_1 |\xi|^2 + O(|\xi|^4)$$

where we find

$$\widetilde{\mathbb{Q}}_0 = \frac{1}{2} \left(\frac{|f_2(p)|}{|f_1(p)|^2} \right)^2$$

and

$$\widetilde{\mathbb{Q}}_1 = \frac{1}{|f_1(p)|^2} \left(\frac{|f_2(p)|^4}{|f_1(p)|^4} \left(\frac{11}{32} - \frac{5}{12} \operatorname{Re} \left[\frac{f_1(p)f_3(p)}{(f_2(p))^2} \right] \right) + \frac{1}{8} \frac{|f_3(p)|^2}{|f_1(p)|^2} \right). \quad (6.27)$$

There are two circumstances under which $\widetilde{\mathbb{Q}} = \widetilde{\mathbb{Q}}_0 = \widetilde{\mathbb{Q}}$. The first, which is the trivial case, is when the lattice spacing $|\xi|$ of the original lattice in the z -plane vanishes. The second case is complex inversion $f(z) = 1/z$ (or more generally a bilinear transformation), for which we find $\widetilde{\mathbb{Q}}_1 = \widetilde{\mathbb{Q}}_2 = \widetilde{\mathbb{Q}}_3 \dots = 0$. The vanishing of all the higher order corrections means that all the curves emanating from the vertex at $f(p)$ are circular arcs. It follows that, for a 2D foam or a quasi 2D foam, Laplace's law is satisfied by each of the arcs.

Let us now turn our attention to the mapping $f(z) = z^{1/2}$ in this case we do not expect Laplace's law to hold for each of the arcs. We have already computed the lowest order term in Eq.(6.27) and found that

$$\widetilde{\mathbb{Q}}_0 = Q = \frac{1}{2R^2}$$

(see Eq.(4.6)). Upon substituting $f(z) = z^{1/2}$ into Eq.(6.27) we find

$$\widetilde{\mathbb{Q}}_1 = \frac{7}{128} \frac{1}{r^3} = \frac{7}{128} \frac{1}{R^6}.$$

where we have transformed from the coordinates in the z -plane (r, λ) to the w -plane coordinates (R, Λ) by using the relationship $\sqrt{r} = R$. Assuming that the original

lattice has a constant lattice spacing $|\xi|$ we can say that a 2D foam, or a quasi 2D foam, is capable of producing a good approximation of a conformal lattice when

$$\widetilde{Q}_1|\xi|^2 = \frac{7}{128} \frac{|\xi|^2}{R^6}$$

is small. We see that this happens at regions a large distance from central (critical) point of the conformal lattice, i.e when $R \gg (7/128)^{1/6}|\xi|^{1/3}$.

Acknowledgements DW acknowledges support from SFI, ESA and CNRS (visiting position at the group of Prof M Adler, Univ. Paris-Est). AM is grateful to Trinity College Dublin and Institute of Mathematical and Physical Sciences, Aberystwyth University, for financial assistance for short visits including the 2007 winter meeting of the British Society of Rheology. AM and DW would like to thank M. A. Moore, S. Cox and W. Drenckhan for advice and useful discussions.

References

- Drenckhan, W., Weaire, D. and Cox, S. J. 2004 The demonstration of conformal maps with two-dimensional foams *Eur. J. Phys.* 25, 429.
- Elias, F., Bacri, J. C., de Mougins, F. H. & Spengler, T. 1999 Two-dimensional ferrofluid foam in an external force field: gravity arches and topological defects *Philosophical Magazine Letters* 79, 389.
- Mancini, M. & Oguey, C. 2005a Equilibrium conditions and symmetries for foams in contact with solid surfaces *Colloids and Surfaces A: Physicochem. Eng. Aspects* 263, 33.
- Mancini, M. & Oguey, C. 2005b Foams in contact with solid boundaries: Equilibrium conditions and conformal invariance *Eur. Phys. J. E* 17, 119.
- Mughal, A. & Moore, M. A. 2001 Topological defects in the crystalline state of one-component plasmas of nonuniform density *Phys. Rev. E* 76, 011606.
- Needham, T. 1997 *Visual Complex Analysis* Oxford University Press.
- Riviera, N., Miri M.F. & Oguey C. 2005 Plasticity and topological defects in cellular structures: Extra matter, folds and crab moulting *Coll. and Surf. A* 263, 39.
- Rothen, F., Pierański, P., Rivier, N. & Joyet, A. 1993 Cristaux conformes *Eur. J. Phys* 14, 227.
- Rothen, F. & Pierński, P. 1996 Mechanical equilibrium of conformal crystals *Phys. Rev. E* 53, 2828.
- Weaire, D. 1999 The equilibrium structure of soap froths: inversion and decoration *Phil. Mag. Lett.* 79, 491.
- Weaire, D. & Hutzler, S. 2001 *The Physics of Foams* Oxford University Press.